30th NENE 2021
September 6 - 9
BLED-SLOVENIA
International Conference Nuclear Energy for New Europe

Preliminary Uncertainty Assessment of a Severe Accident Scenario Using the ASYST Code

Siniša Šadek, Davor Grgić
University of Zagreb, Faculty of electrical engineering and computing
Unska 3
10000 Zagreb, Croatia
sinisa.sadek@fer.hr, davor.grgic@fer.hr

Chris Allison
Innovative Systems Software
3585 Briar Creek Lane
Ammon, Idaho 83406, USA
issgml97@gmail.com

ABSTRACT

The ASYST code, developed as part of an international nuclear technology ASYST Development and Training Program (ADTP) managed by Innovative Systems Software (ISS) is an advanced analysis software for nuclear safety applications. It uses best-estimate SAMPSON THA two-fluid, non-equilibrium models and correlations for thermal hydraulic calculation, SCDAPSIM models for calculation of severe accident progression in the reactor core, and SCDAPSIM COUPLE module for the finite element thermal analysis of the reactor vessel lower head filled with molten corium and a variety of other member-developed computational packages. One of these packages is an integrated uncertainty package developed jointly by the Technical University of Catalunya and ISS. The uncertainty analysis enables the user to perform and post-process multiple computer runs to estimate uncertainty bands for desired output parameters. The code generates automatically the file with sampled values of the input parameters, based on the probability density function, the appropriate percentile and confidence levels (typically using the default Wilks' formula).

The uncertainty analysis is performed for a postulated severe accident scenario of a station blackout at a PWR plant. There are large uncertainties present in the severe accident issues, related to, among others, hydrogen generation during reflood or melt relocation into water, core coolability, in-vessel heat transfer in a damaged core, in-core molten pool behaviour, corium relocation to the lower head, lower head corium behaviour, vessel failure and material release, etc. Some of these issues are taken into account when determining the appropriate SCDAPSIM parameters to be modified and their probability density functions. The objective of the analysis is to determine uncertainty limits of the most important parameters for assessing the core integrity, quantify deviation of results and perform sensitivity study for hydrogen release.

1 INTRODUCTION

Sensitivity and uncertainty analyses have been commonly used for some time in the safety assessment of nuclear power plants (NPP). However, there are many more applications in the field of thermohydraulic analyses and less in the severe accidents area, [1-5]. The quantification of uncertainty as a complement to the best estimate code application is the preferred way for licensing calculations for light water reactors. Conservative calculations may be physically unrealistic due to superficial assumptions and the safety margins thus calculated will not be entirely reliable [2]. The use of best estimate codes with realistic initial and boundary conditions, free from deliberate pessimism, provides a realistic estimate of the overall response of the NPP during an accident. When it comes to severe accidents it is difficult to talk about best estimate practices due to many ambiguities in the core damage process and containment behaviour. This is especially pronounced in parametric codes that use many user-defined parameters. However, mechanistic codes such as RELAP/SCDAPSIM [6] and ASYST [7-10] also partly use correlations that require the external input of certain parameters. There is a limited number of parameters that may affect the results and their influence is tested in the scope of the presented analysis.

The ASYST integrated uncertainty package is based on BEPU (best estimate plus uncertainty) methodology with probabilistic propagation of input uncertainty [11]. The following steps are part of the uncertainty analysis described in this paper:

1. Selection of the plant, nodalization and the accident scenario,
2. Identification of the relevant phenomena and appropriate code parameters,
3. Selection of probability density function (PDF) and random sampling of selected input parameters,
4. Performing multiple calculations determined by the percentile and confidence level using Wilks' formula,
5. Post-processing of results, determination of uncertainty bands, quantification of dispersion of output values and determining the relationship between input and output variables by calculating regression coefficient.

The scenario chosen is a severe accident and the input parameters that vary are related to oxidation and hydrogen production, fuel integrity, material interaction and fuel rod geometry. In this way, the steady state and the early phase of the transient are unchanged, while the deviation in the output results occurs only after the evaporation of water in the core, increase in temperature and start of core degradation.

2 PWR PLANT MODEL AND PREPARATION OF INPUT DATA

2.1 ASYST THA Thermal Hydraulic Nodalization of the Plant

The plant model is based on NPP Krško, a two-loop PWR plant of Westinghouse design. The nodalization of the plant, including the radial cross-section of the core is shown in Figure 1 [12]. Core fuel assemblies, 121 in total, are divided in five regions by grouping similarly powered fuel assemblies together. The ASYST THA model, which is input-compatible with RELAP5/SCDAPSIM, consists of 554 thermal hydraulic volumes, 641 junctions, 361 heat structures with 1923 mesh points, 748 control variables, 197 variable and 221 logical trips. SCDAPSIM components are used for representation of fuel rods, control rods, the core baffle, grid spacers and the structures in the upper plenum. The reactor pressure vessel (RPV) wall in the lower head is modelled using the COUPLE code, a two-dimensional, finite element heat conduction code incorporated in SCDAPSIM.

2.2 Determination of Uncertain Parameters and their Distributions

The uncertainty analysis is based on user defined parameters, grid spacer and fuel rod properties. User defined uncertain parameters include oxide layer stability parameters, metallic meltdown parameters, molten pool parameters, core fragmentation parameters, gamma heating and cladding deformation parameters. Grid spacer uncertain parameters include mass, height, plate thickness and contact radius between the spacer and the fuel rod cladding. The fuel rod uncertain parameters include fuel rod dimensions and plenum geometry data, fraction of theoretical fuel density and helium gas inventory. They are related to SCDAPSIM severe accident module because the intention of the calculation is focused on the core damage progression uncertainty evaluation.

A detailed description of uncertain parameters, a total of 23, and their PDFs is given in Table 1. Parameters for which there are no strict constraints are described by a normal distribution, while parameters for which there are developer recommendations or are limited by the core design are described by a uniform distribution. The mean value and standard deviation are the required data inputs for the parameters described by the normal distribution, while the minimum and maximum values are required for the parameters described by the uniform distribution.

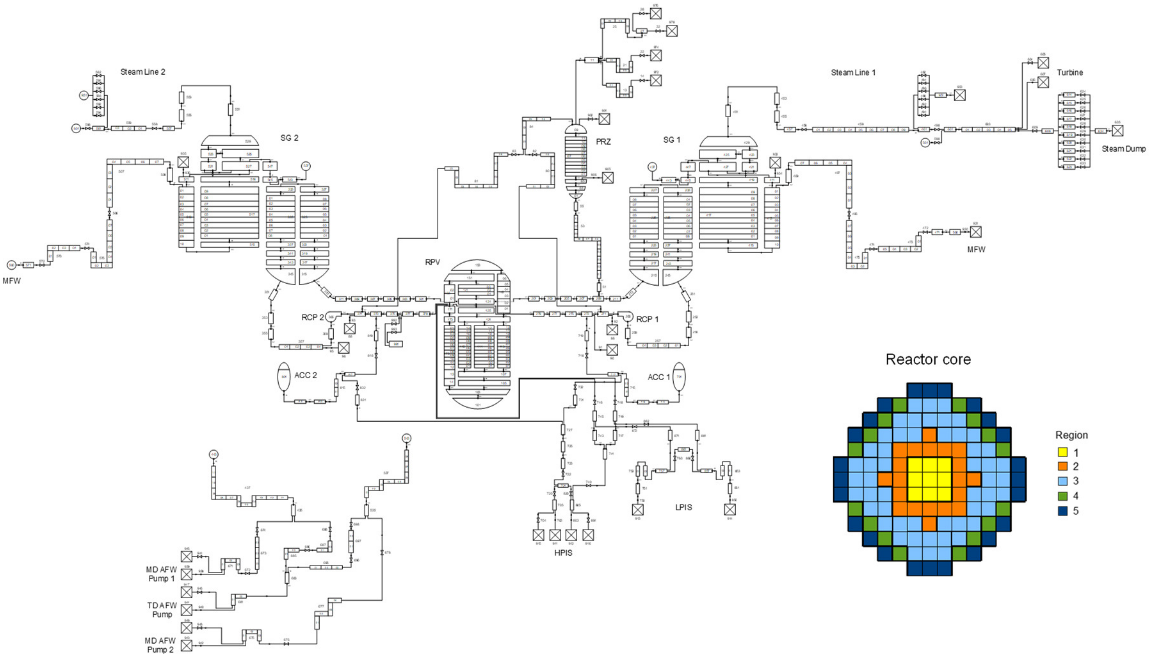

Figure 1: ASYST nodalization of NPP Krško

2.3 Calculation Procedure and Transient Selection

The number of code runs is determined by Wilks' formula. This number depends on the order, percentile and the confidence level [11]. It is decided that Wilks' first order is used with 95% percentile and 95% confidence level, which is a standard procedure for a preliminary analysis. The number of successful code runs is then 59. For example, if the analysis was performed at Wilks' third order with 95% percentile and confidence levels, then the number of calculations required would be 124. In our case 101 calculations were performed because 42 of them failed before the end of the transient time. All calculations have passed the design basis phase and the unsuccessful runs failed when the core degradation started or later during the corium relocation.

The analysed transient is a station blackout in which there is a loss of electric power supply and the opening of breaks at both cold legs at the same time. The break size is 18 mm, a small break LOCA scenario. The transient lasts 20000 s which is preceded by the 1000 s steady state calculation. The transient time is long enough to cover the entire sequence of events for an in-vessel phase of a severe accident, including the late phase of corium accumulation in the lower head, for all valid calculations.

Table 1: Input uncertain parameters

No.	Parameter	Description	Probability density function
1	TFOL	Temperature for failure of oxide layer on the outer cladding surface Default value is 2500 K	Normal distribution with a standard deviation 1% avg.
2	FOSO	Fraction of oxidation of fuel rod cladding for the stable oxide layer Default value is 0.2	Normal distribution with a standard deviation 1% avg.
3	HSDO	Hoop strain threshold for double-sided oxidation Default value is 0.07	Normal distribution with a standard deviation 1% avg.
4	FSDB	Fraction of surface area covered with drops that results in blockage that stops local oxidation Default value is 0.2	Normal distribution with a standard deviation 1% avg.
5	STFD	Surface temperature for freezing of drops of liquefied fuel rod cladding Default value is 1750 K	Normal distribution with a standard deviation 1% avg.
6	VDCM	Velocity of drops of cladding material slumping down outside surface of the fuel rod Default value is 0.5 m/s	Normal distribution with a standard deviation 1% avg.
7	MFFC	Multiplication factor on fuel pellet diameter that defines minimum thickness that crust must have in order to support the molten pool Default value is 1	Normal distribution with a standard deviation 1% avg.
8	TSFQ	Temperature above saturation at which rod fragmentation occurs during quench Default value is 100 K	Normal distribution with a standard deviation 1% avg.
9	GMHF	Gamma heating fraction Default value is 0.026	Normal distribution with a standard deviation 1% avg.
10	RSCR	The strain at which the cladding will rupture Default value is 0.18	Uniform distribution within a range ±1% avg.
11	TSTD	The strain for transition from sausage type deformation to localized deformation Default value is 0.2	Uniform distribution within a range ±1% avg.
12	SLRC	Strain limit for rod-to-rod contact Default value is 0.22	Uniform distribution within a range ±1% avg.
13	MGRS	Mass of grid spacer per fuel rod Default value is 0.00323 kg	Normal distribution with a standard deviation 1% avg.
14	HGRS	Height of grid spacer Default value is 0.03358 m	Normal distribution with a standard deviation 1% avg.
15	PTGS	Plate thickness of grid spacer Default value is $4 \cdot 10^{-4}$ m	Normal distribution with a standard deviation 1% avg.
16	RCGC	Radius of contact area between the grid spacer and the fuel rod cladding Default value is 0.00339 m	Normal distribution with a standard deviation 1% avg.
17	PLLN	Fuel rod plenum length Default value is 0.1864 m	Normal distribution with a standard deviation 1% avg.
18	PLVV	Fuel rod plenum void volume Default value is $9.56 \cdot 10^{-6}$ m^3	Normal distribution with a standard deviation 1% avg.
19	FPLR	Fuel rod pellet radius Default value is 0.004096 m	Uniform distribution within a range 0-0.5% avg.
20	ICLR	Fuel rod inner cladding radius Default value is 0.004178 m	Uniform distribution within a range 0-0.5% avg.
21	OCLR	Fuel rod outer cladding radius Default value is 0.00475 m	Uniform distribution within a range 0-0.5% avg.
22	FFDN	Fraction of fuel theoretical density Default value is 0.95	Uniform distribution within a range ±1% avg.
23	HGFM	Helium inventory in a fuel rod Default value is $6.2 \cdot 10^{-5}$ kg	Normal distribution with a standard deviation 1% avg.

The course of the accident is well known. After the loss of electric power and opening the breaks, the coolant is released from the reactor coolant system (RCS) and the pressure is decreasing. The loss of the secondary heat sink and the termination of natural circulation cause the pressure to rise again, until the moment of loop seal clearing, when it finally begins to decrease. Since there is no emergency core cooling system available, except for the accumulators, water starts to boil causing decrease in heat removal from the core. The core heat up is additionally supported by the fuel cladding oxidation. As the temperature rises, chemical reactions begin, iron-zirconium, nickel-zirconium, silver-zirconium, etc. They lead to liquefaction and melting of fuel assemblies and core supporting structures. The initial melting of local character will eventually grow into the creation of a molten pool. In the final stage of the in-vessel accident progression there is a relocation of the molten material to the lower head. The corium level will increase over time and thermally and mechanically load the reactor vessel wall. The rupture of the wall is not taken into account because it occurs as early as a few hundred seconds after the beginning of the relocation. The idea is to follow in the long run the outflow of corium because there is great scattering among the results, which is described in the next section.

3 RESULTS

Figures 2–8 show the results of the base case and all 59 analyzed cases with variation of input parameters. Thermal hydraulic variables: reactor coolant system pressure, collapsed water level in the core and RCS mass are shown in Figures 2–4, respectively. Variables describing the course of the severe accident: maximum core temperature, production of hydrogen, radius of corium in the core and corium height in the lower head are shown in Figures 5–8, respectively.

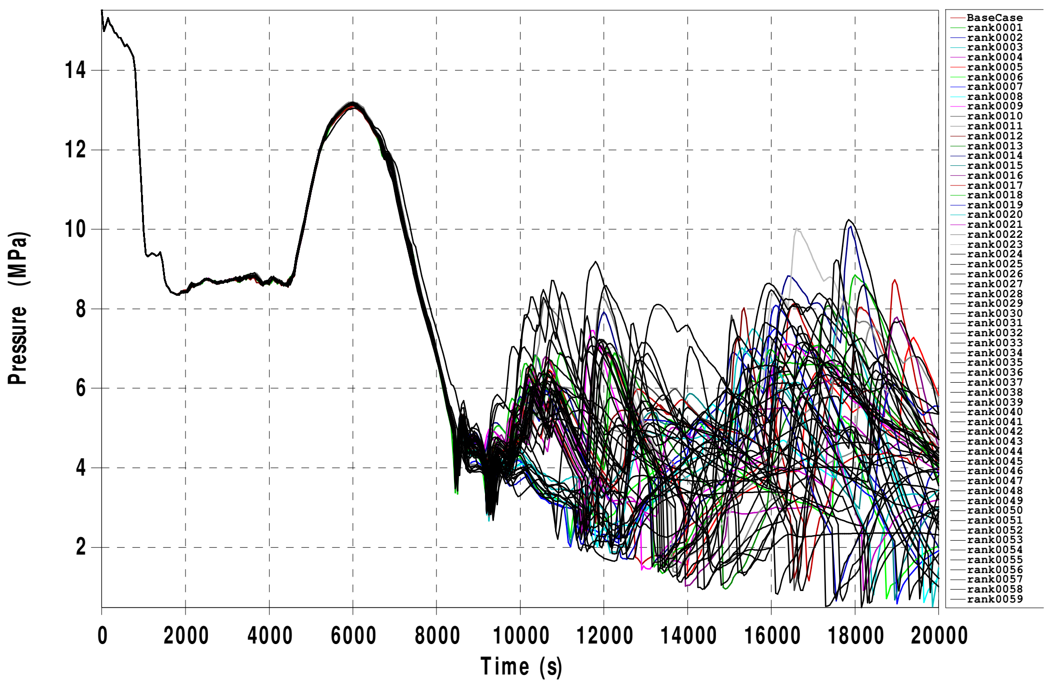

Figure 2: Pressurizer pressure

The results of the steady state are not shown because the changes in the parameters do not affect the behaviour of the power plant in normal operation. In fact, there is no visible deviation in the results until 9000 s. At that point, the maximum core temperature already reaches the value at which the liquefaction of oxide materials, ZrO_2 and UO_2, begins. The mass of hydrogen produced is at 70% of total production, the RCS is heavily depleted and the core is dried out. The major change in results occurs after the relocation of the corium from the core to the lower head.

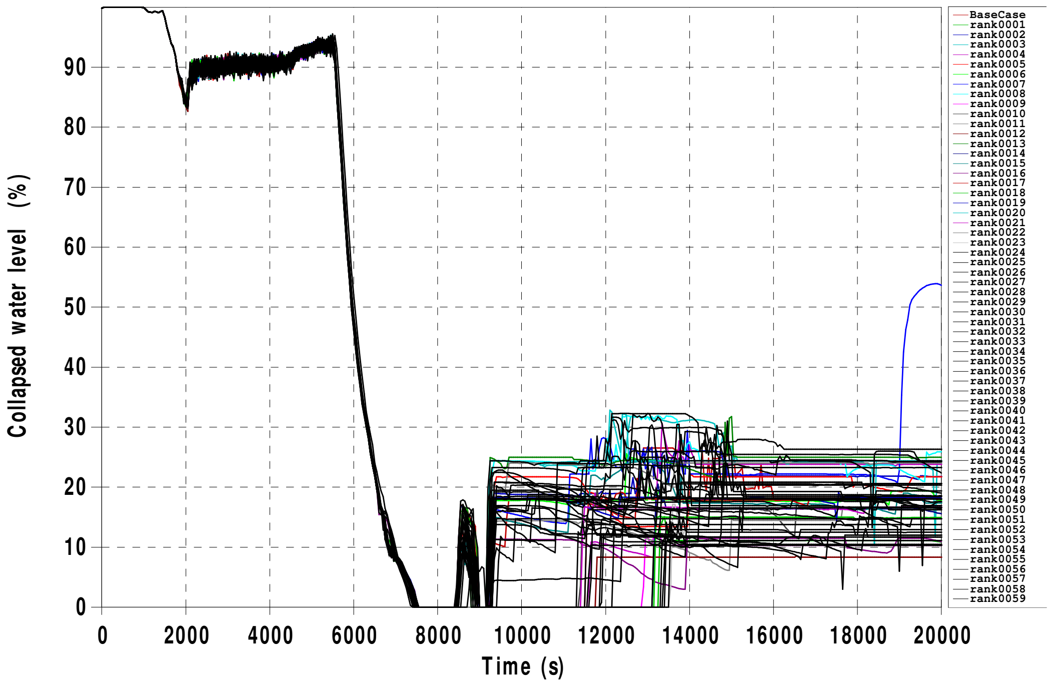

Figure 3: Collapsed water level in the core

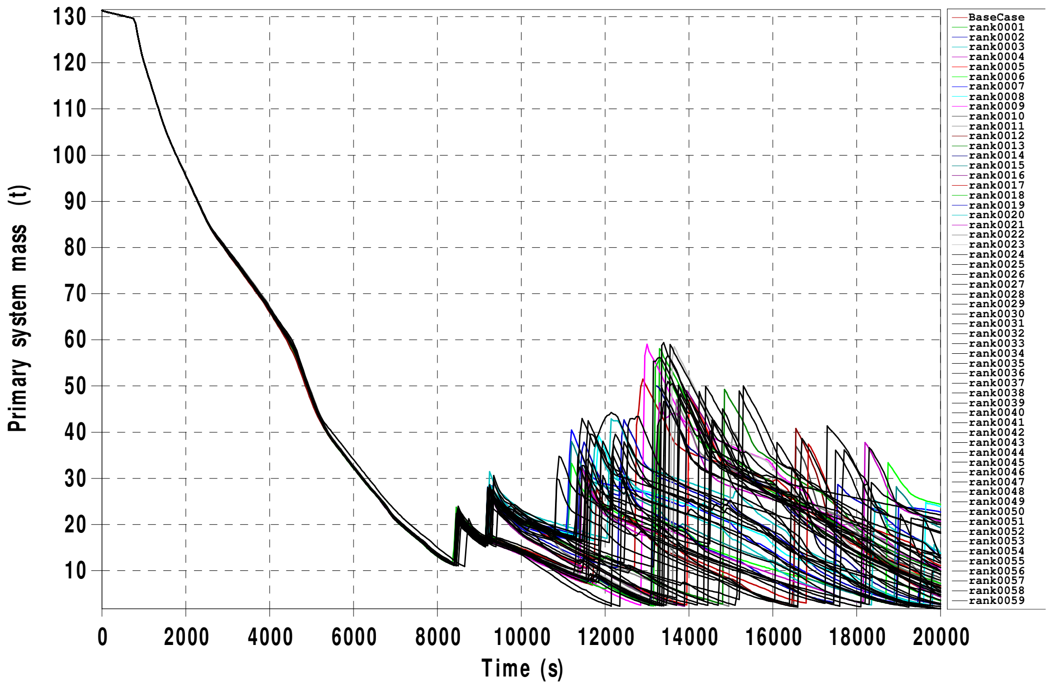

Figure 4: Primary system mass

Scenarios that predict earlier relocation result in higher primary pressure. The increase in pressure is due to the evaporation of water in the lower plenum after the pouring of hot material. If the pressure is higher than 5 MPa, the accumulators will not be activated and the core damage will not be slowed down. This means that the later course of the accident will be significantly different depending on the moment of initial melting of the structure or the crust supporting the molten pool.

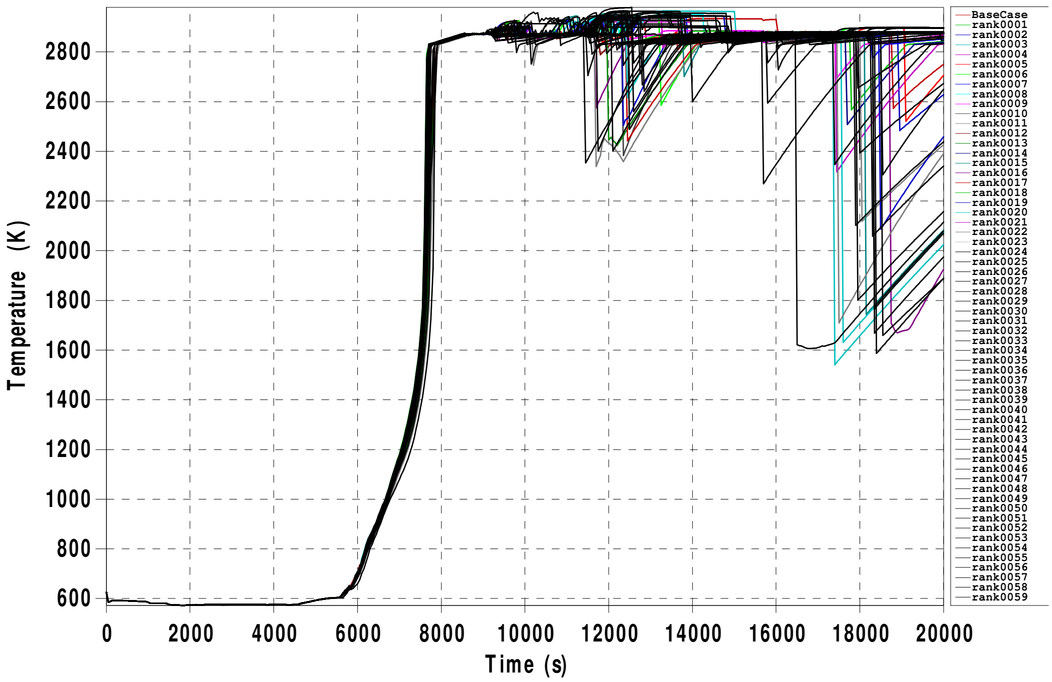

Figure 5: Maximum core temperature

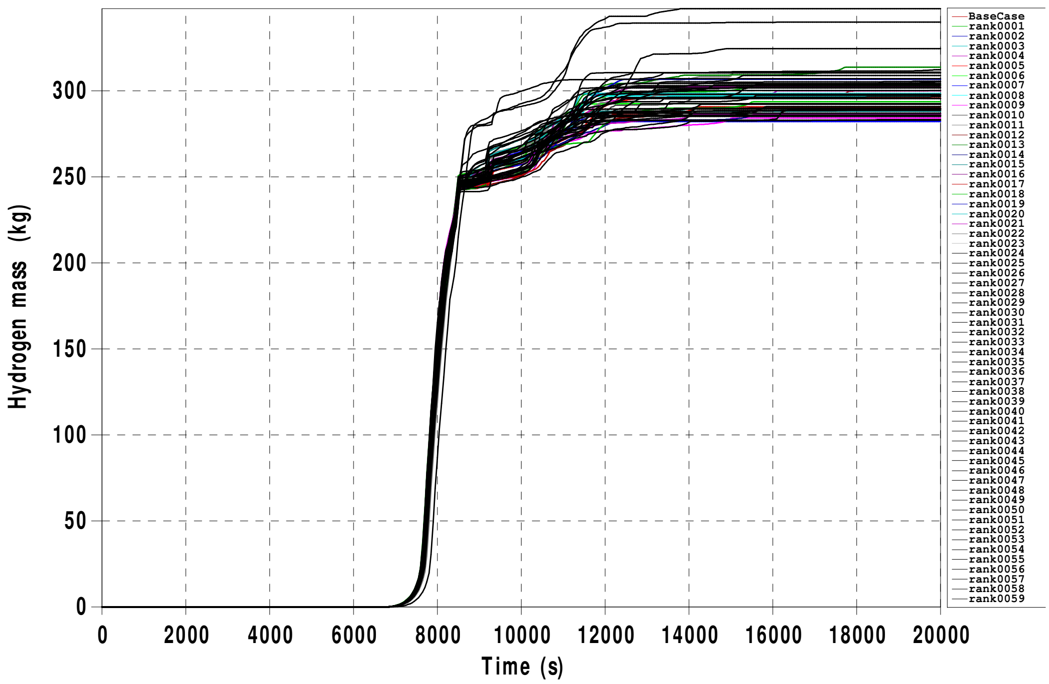

Figure 6: Hydrogen production

Variations in the behaviour of the primary pressure are the result of evaporation of water injected from the accumulators or the previously mentioned evaporation in the lower plenum. The accumulator operation can be observed in figures representing the core level and the RCS mass, Figure 3 and Figure 4, due to the sharp increase in the value of these variables. Production of hydrogen and core maximum temperature are less affected by the corium relocation. The majority of hydrogen is produced while the core is still intact, and the temperature rises due to reduced heat removal, as the water in the core boils, and release of heat during oxidation. A closer look at some scenarios shows that the total amount of hydrogen is lower in the cases where relocation occurs earlier because then the accumulators inject less water, whose evaporation would otherwise enhance oxidation and hydrogen production. This is especially manifested in the later phase of the accident.

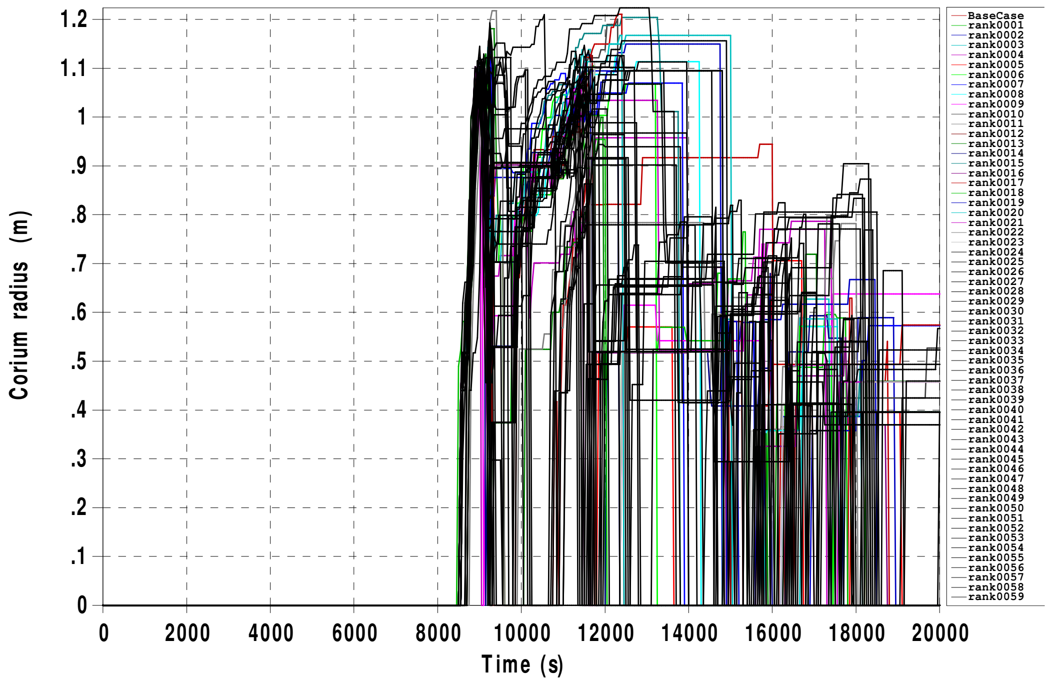

Figure 7: Radius of the in-core molten pool

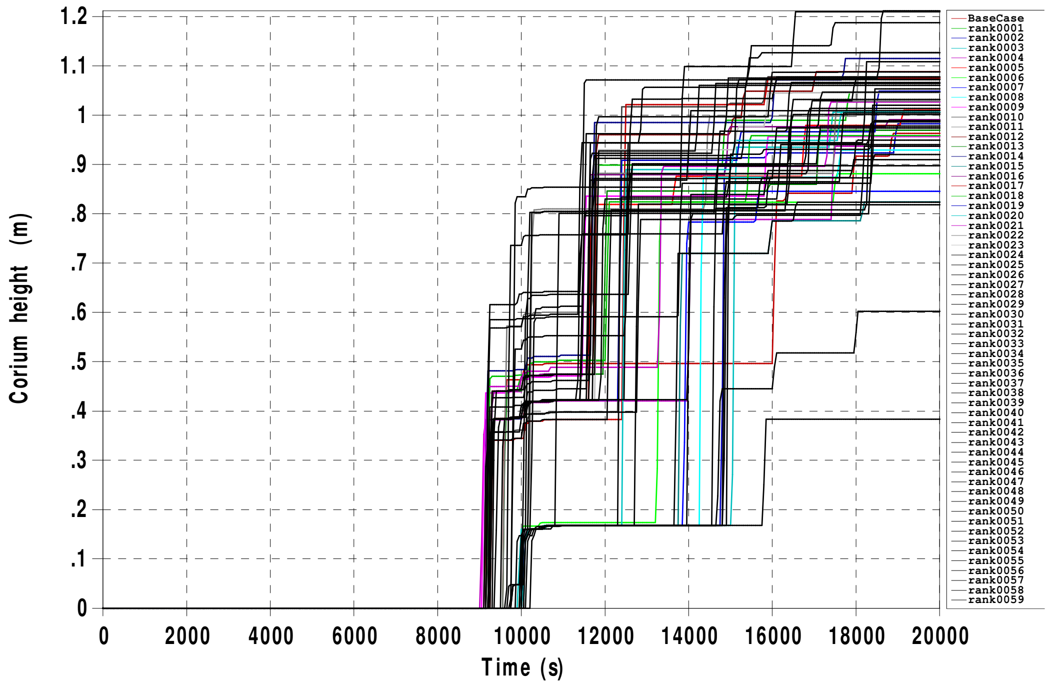

Figure 8: Corium height in the lower head

Corium leakage and in-core pool emptying significantly affect both thermohydraulic behaviour and the progression of a severe accident. Although the time deviation of this event among the different scenarios is only 10-100 s, the further course of the accident changes greatly, quantitatively and qualitatively. Before that, the results do not differ qualitatively too much, especially as long as the geometry of the core is preserved.

The stability of a crust surrounding the molten pool is a function of several variables, including the thickness of the crust and the differential pressure between the fluid inside the crust and the fluid outside of the crust. If the molten pool is surrounded by reactor coolant that is considerably cooler than the liquidus temperature of the material in the molten pool, then a thick crust will form around the pool and hold it in place. If the coolant surrounding the molten pool is at about the same temperature as the liquidus temperature of the material in the molten pool, then the crust surrounding the molten pool will be thin. If the crust is thin or the stresses in the crust are large relative to its ultimate strength, then the crust may fail and thus remove a constraint on spreading of the molten pool. Variations in the input parameters affect the fuel and coolant temperatures, as well as the differential pressure around the crust. These variations do not need to be large for crustal cracking to occur, and this is why some scenarios result in earlier relocation. The significant variations in results representing radius of corium in the core and corium height in the lower head are due to different cracking times of the crust.

4 DISCUSSION

4.1 Dispersion of Results

Statistical analysis is used to determine the scatter of results using the relative standard deviation (RSD). The RSD is defined as a ratio between standard deviation and population mean value:

$$RSD = \sqrt{\frac{1}{N}\sum_{i=1}^{N}\left(\frac{x_i}{\overline{x}} - 1\right)^2}\ , \qquad (1)$$

where N is the size of the population, x_i i-th population value, and $\overline{x}$ the population mean. Relative standard deviations of thermal hydraulic variables: collapsed water level (CORWAT), RCS mass (RCSMASS), break flow rate (BRKFLRAT), integral break flow (BRKFLINT), pressurizer (PRZPRES) and accumulator (ACCPRES) pressures are shown in Figure 9, while for SCDAPSIM variables: maximum core temperature (BGMCT), production of hydrogen (HYDR), corium height in the lower head (HGTCOR) and radius of in-core molten pool (REPOOL), are shown in Figure 10. The largest scattering among thermohydraulic variables is recorded for the break flow rate, followed by the primary system mass. Due to the different accumulator discharge times, there are several peaks for the core water level deviation in the period from 7000 s to 9000 s, but globally the RSD is relatively small. The peaks are also observed for the deviations of SCDAPSIM variables because of different starting times of hydrogen production and corium degradation. Interestingly, the variables that directly describe core degradation have less scatter although most of the input varying parameters are predominately related to them. The only exception is the deviation of a radius of the in-core molten pool for the reasons described earlier.

Table 2 shows mean values of relative standard deviation and coefficient of range, as well as their maximum values, for output variables. The coefficient of range is defined as the ratio of difference between the highest and the lowest value of a variable to their sum, $(x_{max} - x_{min})/(x_{max} + x_{min})$.

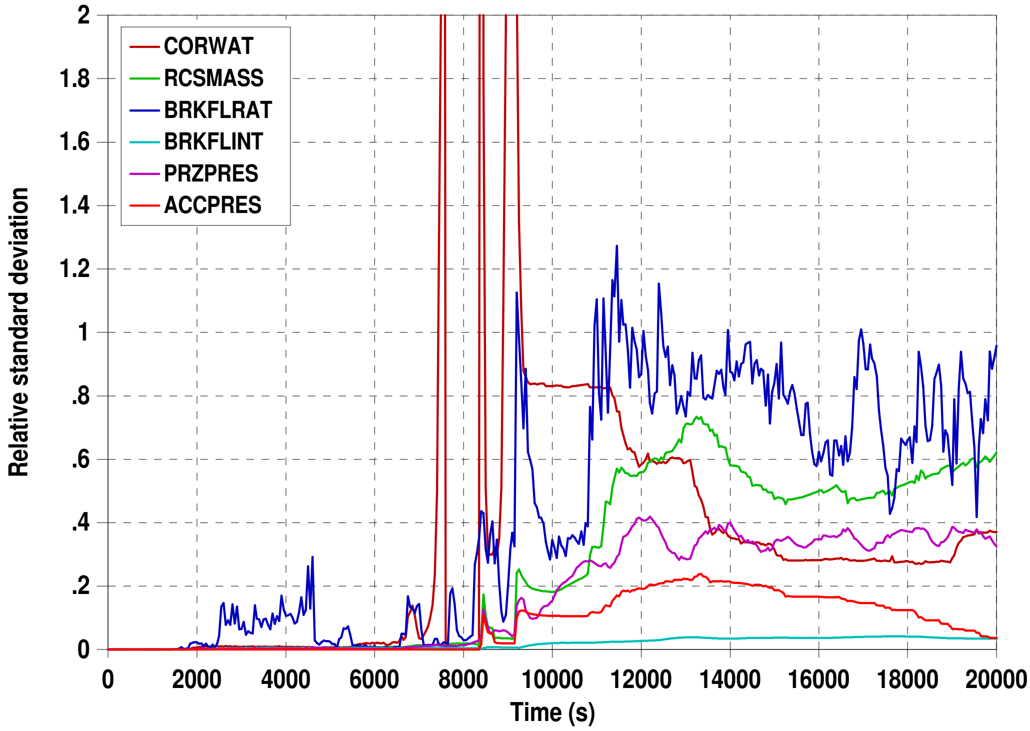

Figure 9: Relative standard deviations for thermal hydraulic variables

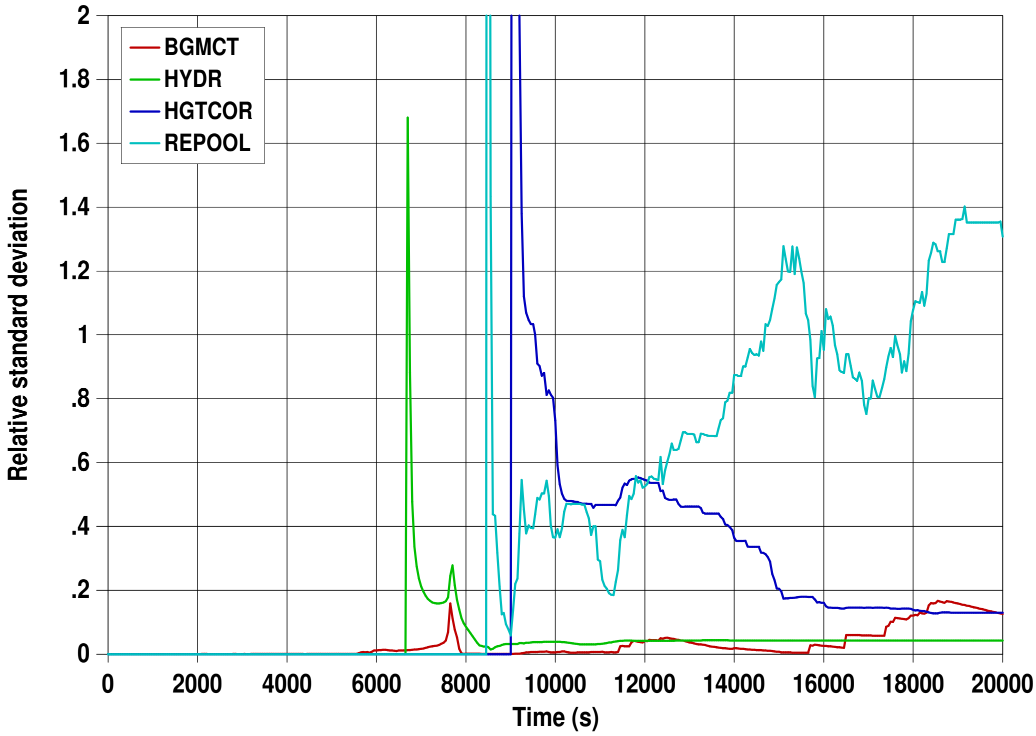

Figure 10: Relative standard deviations for SCDAPSIM variables

Table 2: Mean and maximum values of relative standard deviation and coefficient of range for output variables

Variable	**Relative standard deviation, mean**	**Relative standard deviation, maximum**	**Coefficient of range, mean**	**Coefficient of range, maximum**
Maximum core temperature	0.04	0.17	0.08	0.30
Production of hydrogen	0.06	1.68	0.16	1.0
Collapsed water level	0.48	7.75	0.52	1.0
RCS mass	0.36	0.73	0.48	0.92
Break flow rate	0.50	1.27	0.56	0.99
Integral break flow	0.02	0.04	0.05	0.10
Corium height in the lower head	0.42	7.75	0.67	1.0
Pressurizer pressure	0.22	0.42	0.40	0.90
Accumulator pressure	0.14	0.24	0.24	0.43
Radius of in-core molten pool	0.83	7.75	0.99	1.0

4.2 Sensitivity Analysis

A linear regression analysis is performed to study the relationship between the input parameters and the output results. For this purpose, the Pearson correlation coefficient *r* given by the following equation is used:

$$r = \frac{\sum_{i=1}^{N}(x_i - \overline{x})(y_i - \overline{y})}{\sqrt{\sum_{i=1}^{N}(x_i - \overline{x})^2 \sum_{i=1}^{N}(y_i - \overline{y})^2}}, \tag{2}$$

where N is the sample size, x_i, y_i the individual sample points indexed with i, $\overline{x}$ and $\overline{y}$ sample means.

Sensitivity analysis is conducted for hydrogen production as one of the most important quantities during a severe accident. In addition, this variable is either constant or increases over time which means that there is a clear correlation with the input parameters. According to equation (2), if the Pearson coefficient is positive, both variables increase or decrease, and if it is negative, one variable increases and the other one decreases. In our case, if the coefficient is positive, hydrogen production increases if the input parameter increases, and if it is negative, hydrogen production increases if the input parameter decreases.

Pearson correlation coefficients describing relationship between input uncertain parameters and hydrogen mass are shown in Figure 11. According to [13] if the coefficient is less than 0.3 absolute, there is a weak correlation between the variables, which is more or less the case for all input variables. There are several parameters that have a weak to medium influence on hydrogen release, which depends on the oxidation rate. The cladding oxidation can be divided in two phases. The first phase refers to an interval of approximately 7000 s to 9000 s and represents the oxidation of the intact core, which takes place at a higher rate. The second phase begins at 9000 s during which oxidation is slower and the core is partially or completely degraded. Parameters like temperature for failure of oxide layer on the outer cladding surface, strain limit for rod-to-rod contact and fraction of fuel theoretical density result with positive coefficient and have a lower impact during the first phase of oxidation and higher during the second phase. Conversely, parameters such as the strain for transition from sausage type deformation to localized deformation and fuel rod plenum length also give positive Pearson coefficient but are higher during the first phase and lower during the second phase. The correlation coefficient is negative for the fuel rod radii meaning that hydrogen production is higher if the fuel dimensions are reduced. Finally, there are parameters that result in a correlation coefficient whose sign changes with the transition from the first to the second oxidation phase. For example, gamma heating fraction and the strain at which the cladding will rupture give a correlation coefficient that is positive during the first phase and negative during the second phase of oxidation, while the opposite is true for the velocity of slumping droplets. The analysis thus reveals a complex correlation between input parameters and hydrogen production.

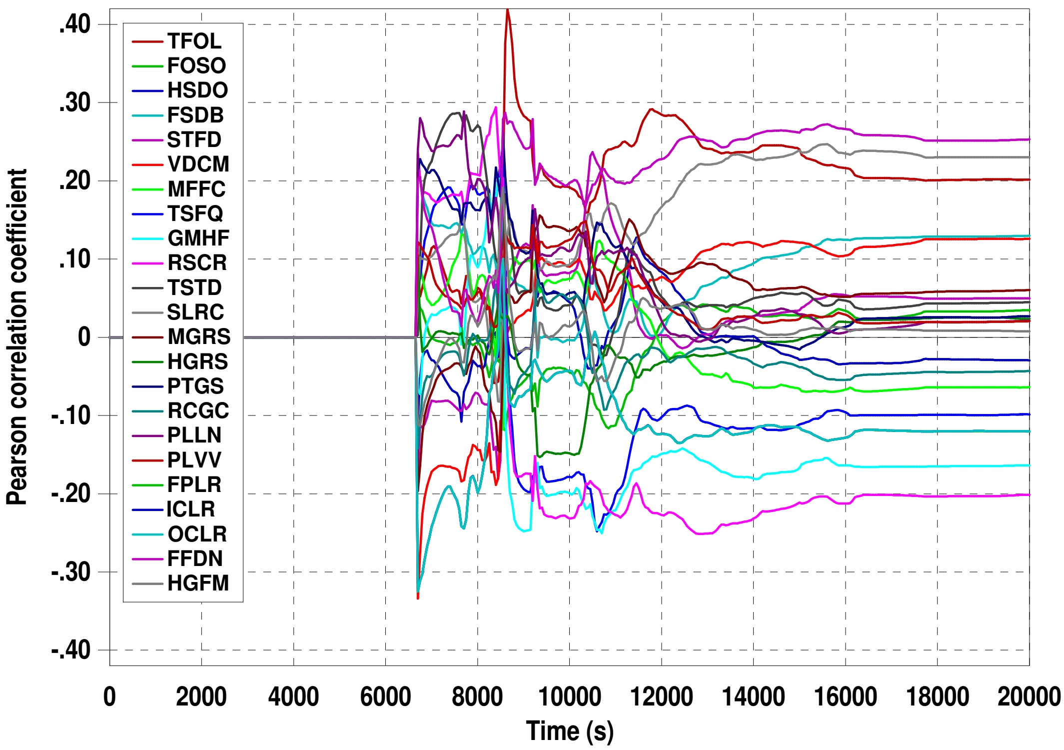

Figure 11: Pearson correlation coefficient between input parameters and hydrogen production

5 CONCLUSION

Small variations in dimensions of fuel and support structures and in values of input parameters related to core damage modelling influence calculation results of nuclear power plant behaviour during a severe accident. The steady state and early transient results, before the start of core melt, deviate only slightly. The formation of an in-core molten pool and, especially, relocation of corium to the lower head are phenomena that significantly affect thermohydraulic and structural core behaviour. Even small differences in the timing of these events in different scenarios greatly change the further course of the accident. In the case of earlier corium relocation there is a sharp increase in primary pressure, accumulators are activated later and the core damage progresses faster. As for hydrogen generation rate and core maximum temperature, their values are less affected by the corium relocation because they are driven by fuel rod cladding oxidation which is more dominant when the fuel rod geometry is still intact. These variables also have the lowest relative standard deviations comparing to other important output parameters. Only the mass of coolant released from the RCS through the break has a smaller deviation. The statistical analysis shows that thermohydraulic variables in general have larger scatter of results than variables describing core degradation.

Sensitivity analysis shows a complex dependence of hydrogen production on the values of input parameters. The Pearson correlation coefficient depends on the phase of the accident; it may have a smaller impact in the initial stage and a larger one in the later stage, or vice versa, and may even change its sign during the oxidation process. A weak correlation is found between the input data and the hydrogen mass which is consistent with a small relative standard deviation of hydrogen release. Some parameters such as temperature for failure of oxide layer and velocity of slumping droplets indicate a medium effect but this occurs during a short period of time at the beginning of the oxidation, or during the initial phase of the in-core molten pool formation.

REFERENCES

[1] Quantifying Reactor Safety Margins – Application of Code Scaling, Applicability and Uncertainty Evaluation Methodology to a Large-Break, Loss-of-Coolant Accident, NUREG/CR-5249, EGG-2552, December 1989.

[2] Report on the Uncertainty Methods Study, NEA/CSNI/R(97)35, Vol. 1 and 2, June 1998.

[3] BEMUSE Phase III Report – Uncertainty and Sensitivity Analysis of the LOFT L2-5 Test, NEA/CSNI/R(2007)4, October 2007.

[4] F. D'Auria, W. Giannotti, "Development of a Code with the Capability of Internal Assessment of Uncertainty", Nucl. Technol., 131:2, 2000, pp. 159-196.

[5] H. Glaeser, "GRS Method for Uncertainty and Sensitivity Evaluation of Code Results and Applications", Sci. Technol. Nucl. Install., Volume 2008, Article ID 798901, 2008.

[6] C. M. Allison, J. K. Hohorst, "Role of RELAP/SCDAPSIM in Nuclear Safety", Sci. Technol. Nucl. Install., Volume 2010, Article ID 524658, 2010.

[7] A. Nakata, M. Naitoh, C. M. Allison, "Need of a Next Generation Severe Accident Code", Tri Dasa Mega, 21(3), 2019, pp. 119–126.

[8] A. Nakata, C. M. Allison, J. K. Hohorst, M. Naitoh, K. Matsubara, R. Pericas, "Development and Preliminary Assessment of the new ASYST Integral Analysis BEPU Code using the PBF SFD-ST Bundle Heating and Melting Experiment, a Typical BWR Under Fukushima-Daiichi-Accident-Like Thermal Hydraulic Conditions and PWR for a Steam Line Break in the Containment", Proc. of ICAPP 2021, October 16-20, 2021 (Virtual).

[9] A. K. Trivedi, D. R. Novog, C. M. Allison, "Implementation of Solar Salt as Fluid in ASYST4.1 and Validation for a Natural Circulation Loop, Proceedings of ICONE 28, August 4-6, 2021 (Virtual).
[10] ASYST THA VER 3 Manuals, Innovative Systems Software, April 2020.
[11] M. Perez, F. Reventos, R. Wagner, C. Allison, "Integrated Uncertainty Analysis using RELAP/SCDAPSIM/MOD4.0", Proc. of the 13th International Topical Meeting on Nuclear Reactor Thermal Hydraulics (NURETH-13), Kanazawa City, Ishikawa Prefecture, Japan, September 27 – October 2, 2009, N13P1252.
[12] S. Šadek, D. Grgić, V. Benčik, Š. Vlahović, "Analysis of the upflow conversion modification and influence on selected LOCA accidents in a PWR plant", Nucl. Eng. Des., 369, 2020, Article ID 110854.
[13] W. Jaeger, V.H. Sanchez Espinoza, F.J. Montero Mayorga, C. Queral, "Uncertainty and Sensitivity Investigations with TRACE-SUSA and TRACE-DAKOTA by Means of Post-test Calculations of NUPEC BFBT Experiments", NUREG/IA-0462, August 2017.